Journal of Engineering Science and Technology Review 14 (5) (2021) 156 - 162

JOURNAL OF
Engineering Science and Technology Review

Research Article

www.jestr.org

Analysis and Control of Single-Phase Grid-Connected Inverter with Inductive-Capacitive-Inductive Filter

Zhuo Meng[1,*], Lei Guo[1,2] and Yize Sun[1]

[1]*College of Mechanical Engineering, Donghua University, Shanghai 201620, China*
[2]*College of Mechanical and Electrical Engineering, Fujian Agriculture and Forestry University, Fuzhou 350100, China*

Received 26 August 2021; Accepted 13 October 2021

Abstract

Owing to the increased penetration of a distributed generation system, a single-phase grid-connected inverter (SPGCI) with inductive-capacitive-inductive (LCL) filter has been widely used in a small-scale power generation system. However, for a grid-connected inverter-based generation system, power quality is affected by the resonance problem caused by LCL filter, and a control strategy is required. To enhance the power quality in a generation system that has SPGGI with an LCL filter, a dedicated control scheme based on grid voltage feedforward (GVFF) and a double-loop control that is composed of capacitor current feedback (CCF) and a proportional-resonant (PR) controller were proposed. CCF-based resonant damping was analyzed on the basis of a mathematical model. The control including PR and GVFF was also analyzed. The feasibility was verified through simulation. Results show that CCF-based active damping can effectively suppress resonant peak, generating a frequency characteristic similar to that of passive damping, but without power loss. The technique composed of double-loop control and GVFF exhibits various strengths, such as high steady-state accuracy and low total harmonic distortion below 5%, ensuring the high quality of injected grid current. This study can offer a reference for the control of SPGCI.

Keywords: Single-phase grid-connected inverter, LCL filter, Active damping, Proportional-resonant control, Feedforward control

1. Introduction

On the one hand, economic development imposes increased energy demands. On the other hand, the extensively used fossil energy could generate various harmful emissions, resulting in environmental pollution [1]. Consequently, using alternative energy to replace or supplement fossil energy has become an urgent problem to be solved. Renewable energy, such as solar energy and wind energy, is abundant and pollution-free and has attracted increasing attention [2]. For solar energy, one main application is its conversion into electrical energy by using a distributed generation system (DGS).

Generally, a small-scale photovoltaic (PV) DGS depends on a single-phase grid-connected inverter (SPGCI) to realize energy conversion, in which the direct current (DC) from a PV panel is converted into alternating current (AC) injected into the grid. Thus, for SPGCI, its performance will greatly influence the overall performance of a generation system. Its control has received increased focus [3]. In SPGCI, a filter is an essential component used to eliminate the switching harmonic introduced by pulse width modulation (PWM). Compared with inductive and inductive-capacitive filters, an inductive-capacitive-inductive (LCL) filter presents better performance in terms of smaller current ripple, higher harmonic attenuation, and smaller volume, and it has become a favorable choice for a grid-connected inverter (GCI) [4]. Nevertheless, the frequency response curve of an LCL filter exhibits a peak at resonant frequency (f_r), resulting in a resonance problem. It can cause oscillation, deteriorate power quality, and even destabilize a system under a severe condition [5]. Therefore, the resonance problem has become a challenge for GCI with an LCL filter.

Consequently, different studies have focused on the control of an LCL-type GCI, and passive damping (PD) methods have been employed [6-9]. Although a PD method can suppress the resonant peak, the damping component will generate power loss, resulting in decreased system efficiency. Thus, for GCI with an LCL filter, resonance should be suppressed to ensure system stability and efficiency, and reference current should be tracked to provide high-quality current injected into the grid.

Accordingly, this study proposes capacitor current feedback (CCF)-based active damping (AD) to suppress resonance. A hybrid method integrated with proportional-resonant (PR) and grid voltage feedforward (GVFF) control is used to enhance power quality. The theoretical analysis and parameter design are given on the basis of mathematical modeling, offering a guideline for the control of SPGCI with an LCL filter.

2. State of the art

Many investigations have focused on the control of GCI with an LCL filter. Xu et al. [10] proposed a split capacitor-based damping method for a three-phase GCI, in which an additional capacitor was connected in parallel with the filter capacitor. This method could realize resonance suppression, gain reduction at high frequencies, and improved filter performance. However, the resistor in series with the filter capacitor would still generate power loss. Xu [11] suggested

*E-mail address: mz_dhu@hotmail.com,leiguocn@hotmail.com
ISSN: 1791-2377
doi:10.25103/jestr.145.18

an AD method by generating a virtual resistor connected in parallel with the filter capacitor branch. The impact of frequency response on the system was analyzed using a mathematical model. The effectiveness was verified through simulation. Although this method could achieve resonant damping, the influence of the virtual resistor value on the damping result was not illustrated. As a result, an inappropriate value might diminish the effectiveness of this method. Yang et al. [12] also proposed a CCF-based method to suppress resonance. A proportional-integral (PI) controller was employed to regulate the output current. The simulation results confirmed its performance. Nevertheless, the PI controller was more suitable for DC signal than AC signal. The controller could not realize zero steady-state error for AC signal. Bierhoff et al. [13] also presented PI approach based control for an inverter with an LCL filter. In accordance with the Nyquist criteria, the parameter range for the PI controller to guarantee system stability was given.

Wu et al. [14] used CCF to damp resonance and applied a PR controller to adjust grid current in a synchronous reference frame, also called dq frame. Its feasibility was ascertained through simulation. However, a single-phase inverter system has no orthogonal signal in a stationary reference frame, also called $\alpha\beta$ frame. Therefore, its realization with coordinate transformation from $\alpha\beta$ frame to dq frame requires artificially constructed orthogonal signal generation, which can be obtained using various phase shift methods. This requirement increases the complexity. Song et al. [15] proposed a state observer based method to resolve the resonance issue. A PI controller was implemented on dq frame. This implementation led to a similar problem, that is, the construction of dq frame. The state observer also increased its complexity. Tang et al. [16] presented decoupling control for d- and q-axis current based on state feedback for SPGCI. Geddada et al. [17] adopted a PI controller on dq frame for a three-phase inverter.

Dang et al. [18] proposed improved sliding mode control with CCF to reduce the total harmonic distortion (THD) of grid current. The performance was assessed via simulation in the MATLAB/Simulink platform. Nonetheless, this method was applied to a three-phase GCI and performed in dq frame. Hence, it could not directly be employed to SPGCI. Zhu et al. [19] suggested a two controller-based scheme, in which one is used to damp resonance by using grid current feedback, and the other one is used to regulate grid current. This approach was only considered for a three-phase inverter. Moreover, two controllers must be implemented in a stationary $\alpha\beta$ frame. Thus, this scheme is unsuitable for SPGCI.

Eldeeb et al. [20] proposed the Kalman filter to estimate capacitor current to suppress resonance, but without current sensor. Despite its merit, this method has complex computation and must obtain the current and voltage in $\alpha\beta$ frame. Li et al. [21] presented a double-loop scheme with capacitor current and grid-side current to control resonant peak. This technique increases the system order. The capacitor current is fed back to input by a PI controller, thereby increasing the burden for parameter design and tuning. Sosa et al. [22] developed an indirect method to suppress resonant peak and regulate injected grid current for GCI with an LCL filter. The main feature of this method is that the injected grid current is indirectly regulated. In fact, its regulation is realized by adjusting inverter-side current on the basis of estimated inverter-side reference current and grid voltage. Theoretical analysis on system stability and error and experimental results were also presented. However, the estimation algorithm for inverter-side current is cumbersome. Parameter variation may cause an increased error of the inverter-side current, thus deteriorating power quality.

Bighash et al. [23] developed a model predictive control (MPC) based method to adjust inverter current. This methodology is robust and is adaptive to grid impedance variation and even LCL filter parameter variation. In its realization, the switching plan and duty cycle are obtained using a cost function and a switching table, respectively. Nevertheless, the cost function computation requires DC bus voltage. An orthogonal signal must be generated for control purpose. Similarly, Young et al. [24] presented an MPC-based technique for controlling a voltage source inverter with an LCL filter. When this method is used, no additional damping is needed. This method asserts less computation time compared with the traditional MPC approach. Irrespective of these strengths, this method could only be applied to inverter running in isolated mode rather than grid-connected mode.

Guzman et al. [25] presented a state observer based model for a three-phase inverter. Resonant damping was implemented only using estimated inverter-side current. Experimental results were provided to substantiate its effectiveness. Benrabah et al. [26] proposed a Pade approximation based model for a three-phase inverter. Active disturbance rejection control was employed to resolve the problem from an LCL filter. Nonetheless, the two proposed methods are complex, and both were applied to a three-phase system. Yang et al. [27] presented the application of capacitor current to resonant damping. Grid current was regulated using a one-cycle control based method. Although the simulation results demonstrated its veracity, this technique is for a Z source inverter. Zheng et al. [28] presented a passivity-based controller for GCI with an LCL filter. The controller parameters were optimized using the particle swarm optimization algorithm. Alamri et al. [29] applied a genetic algorithm to optimize the LCL filter parameter for a multilevel inverter. Simulation analysis was conducted in the MATLAB/Simulink platform.

The above studies have presented several main issues, such as power loss, control realization in dq or $\alpha\beta$ frame instead of a natural frame, a relatively large steady-state error, and relatively complex control algorithms. By contrast, the CCFAD method features simplicity and effectiveness. The PR controller can eliminate steady-state error when it is applied to AC signal. Under such context, this study recommends a hybrid method with CCFAD and PR to control SPGCI with an LCL filter. GVFF is added to facilitate control performance.

The rest of this study is organized as follows. Section 3 describes the system of SPGCI with an LCL filter. Its mathematical modeling, control scheme, and parameter design are also presented. Section 4 provides the simulation result to verify the proposed method. Lastly, the conclusion is drawn in Section 5.

3. Methodology

3.1 Single-phase grid-connected mathematical model

Fig. 1 shows the system diagram for SPGCI with an LCL filer. V_{dc} represents the DC power, which can be from a DC power supply or renewable energy, such solar energy or wind energy. The four power switches, namely, S1, S2, S3, and S4, are together to form a full-bridge circuit with a function to convert DC into AC. The LCL filter is located between the inverter and grid. Its function is to impede the harmonic from the inverter. L_1 and L_2 are the inverter- and grid-side inductance, respectively. Both equivalent series resistances are neglected. C is the filter capacitor. L_g and R_g are the grid inductance and resistance, respectively. V_{pcc} denotes the point of common coupling, and V_g is the grid voltage.

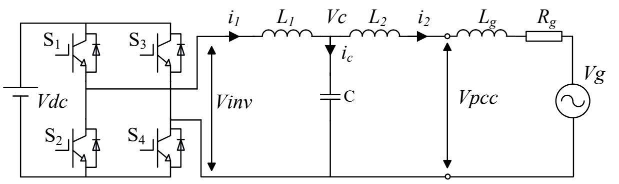

Fig. 1. System diagram of SPGCI with an LCL filter

Assuming that the grid is ideal, L_g and R_g are ignored. Thus, on the basis of the KVL law, the LCL filter can be expressed as the following differential equation:

$$\begin{cases} V_{inv} = L_1 \dfrac{di_1}{dt} + V_c \\ V_c = L_2 \dfrac{di_2}{dt} + V_g \\ Vc = \dfrac{1}{C}\int i_c dt \\ i_1 = i_2 + i_c \end{cases} \tag{1}$$

where V_{inv} is inverter output voltage, V_c is voltage of filter capacitor voltage, i_1 and i_2 are inverter- and grid-side current, respectively.

Eq. (1) can be transformed into s domain via Laplace transformation. The derived block diagram for an inverter with an LCL filter is shown in Fig. 2, where V_{mod} denotes the inverter modulation signal, and *Ginv* represents the sinusoidal PWM. Given that the switching frequency (f_{sw}) of the inverter is much higher than that of the grid (f_0), the PWM inverter can be approximated as

$$G_{inv}(\mathrm{s}) = K_{pwm} = V_{dc} / V_{tri} \tag{2}$$

where V_{dc} is the DC voltage, and V_{tri} is the triangular carrier peak.

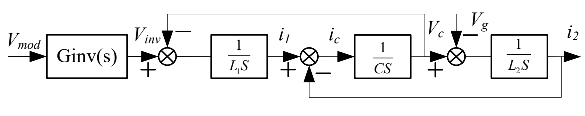

Fig. 2. Block diagram of an inverter with an LCL filter

3.2 Resonance problem of an LCL filter

The transfer function of the LCL filter in Fig. 2, that is, the transfer function of i_2 with respect to V_{inv}, can be expressed as Eq. (3), and the resonant frequency and angular frequency (ω_r) are written as Eq. (4).

$$G_{LCL}(\mathrm{s}) = \frac{1}{s^3 L_1 L_2 C + s(L_1 + L_2)} \tag{3}$$

$$f_r = \frac{\omega_r}{2\pi} = \frac{1}{2\pi}\sqrt{\frac{L_1 + L_2}{L_1 L_2 C}} \tag{4}$$

Fig. 3 plots the bode diagram for the transfer function of i_2 with respect to V_{mod}. The amplitude-frequency curve has a peak at f_r. At the same frequency, the phase-frequency curve has a step change from −90° to −270°. As mentioned before, this peak may lead to oscillation and even system instability, causing a difficulty in current regulation. Consequently, the resonant peak should be suppressed.

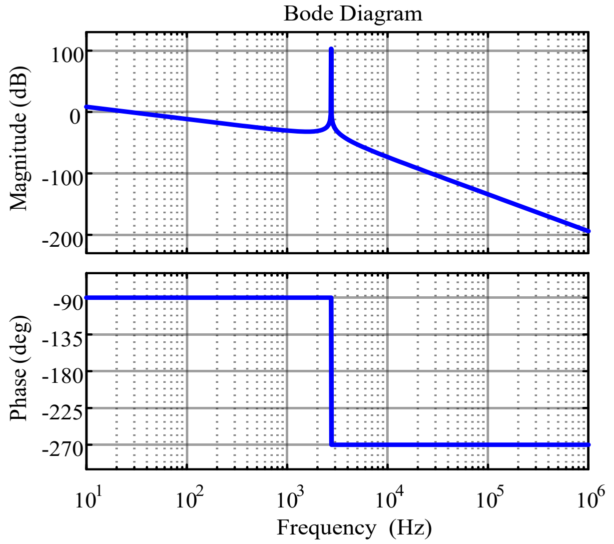

Fig. 3. Bode diagram of the LCL filter

3.3 Double loop with GVFF control

To illustrate the proposed method, the PD based on inserting R_d in series with the filter capacitor C is first explained. Its model is shown in Eq. (5), and the bode diagram with different values of R_d is plotted in Fig. 4. The resonant peak is evidently diminished as the value of R_d is increased. The larger the value of R_d is, the better the damping is. However, R_d will lead to low power. A positive correlation exists between R_d and power loss. This aspect is one of the main disadvantages for such a PD method.

$$G_{LCL\_R_d}(\mathrm{s}) = \frac{sCR_d + 1}{s^3 L_1 L_2 C + s^2 (L_1 + L_2) C R_d + s(L_1 + L_2)} \tag{5}$$

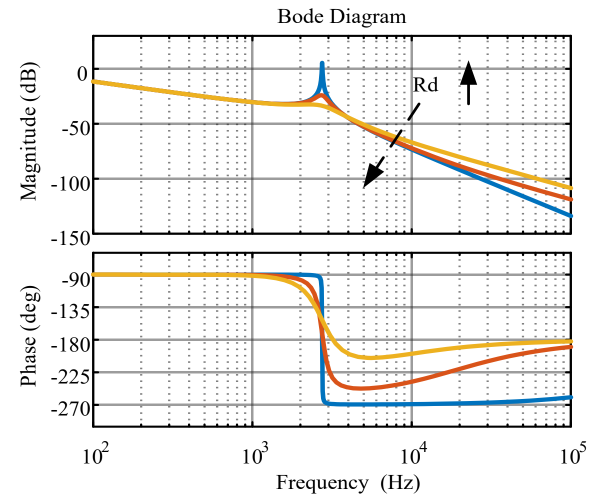

Fig. 4. Bode diagram of PD for an LCL filter for different R_d

Accordingly, this study adopts a double-loop control strategy consisting of CCF and a PR controller to damp resonance and regulate injected grid current. The control of GVFF is also added. Fig. 5 depicts the block diagram, where G_{ff} represents the GVFF gain and can be approximated as $1/K_{pwm}$ [30], K_c is the damping gain, and $G_i(s)$ is the current controller proposed by means of PR. An ideal PR controller can be written as follows:

$$G_{PR}(s) = Kp + \frac{Kr * s}{s^2 + \omega_0^{\ 2}} \tag{6}$$

where K_p and K_r denote the proportional and resonant gains, respectively. ω_0 is the resonant frequency. In theory, an ideal PR controller has an infinite gain at ω_0, which can eliminate steady-state error. Nonetheless, the gain at other frequencies is zero. In other words, the control bandwidth is insufficient. Consequently, an ideal PR controller cannot guarantee high performance when grid frequency fluctuates. Thus, a nonideal PR, also called quasi-PR, is applied to address this defect. Its mathematical expression is as follows:

$$G_{PR}(s) = K_p + \frac{2K_r\omega_c s}{s^2 + 2\omega_c s + \omega_0^{\ 2}} \tag{7}$$

where ω_c is the resonant bandwidth.

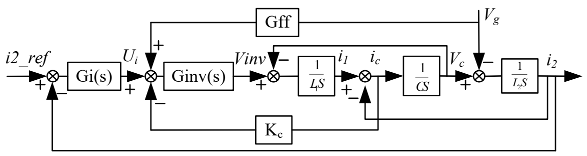

Fig. 5. System block diagram for GCI with CCFAD

3.4 Double-loop parameter design

For further analysis, Fig. 5 can be equivalently transformed into Fig. 6, where G1 and G2 are Eqs. (8) and 9, respectively. The control scheme is a double-loop structure, in which the inner loop is a resonant loop, and the outer loop is a current loop. Usually, for such a double loop, the dynamic response of the inner loop is faster than that of the outer loop. Thus, the parameter of the inner loop should be designed first.

$$G_1(s) = \frac{K_{pwm}}{s^2 L_1 C + sK_{pwm}K_c C + 1} \tag{8}$$

$$G_2(s) = \frac{s^2 L_1 C + sK_{pwm}K_c C + 1}{s^3 L_1 L_2 C + s^2 K_{pwm} K_c L_2 C + s(L_1 + L_2)} \tag{9}$$

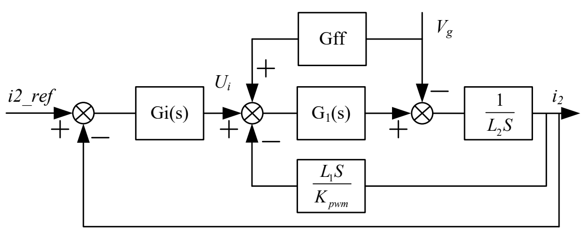

(a)

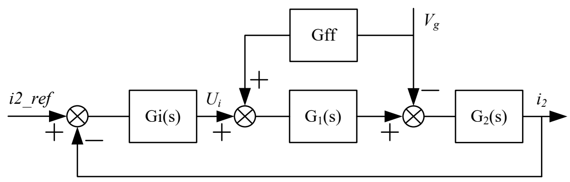

(b)

Fig. 6. Equivalent block diagram for GCI with CCFAD

(1) CCFAD parameter design

The task of parameter design for CCFAD is to determine the damping gain K_c. V_g can be neglected as it is a disturbance signal. Hence, the transfer function of i_2 with respect to U_i can be expressed as follows:

$$G_{LCL\_CCF}(s) = \frac{K_{pwm}}{s^3 L_1 L_2 C + s^2 K_{pwm} K_C L_2 C + s(L_1 + L_2)} \tag{10}$$

Fig. 7 illustrates the bode diagram for G_{LCL_CCF} with different K_c. The resonant peak decreases as K_c increases. This trend is similar to that of the PD method. The proposed AD and PD can suppress resonant peak, improving system stability. Nevertheless, the proposed AD only introduces capacitor current as a feedback variable, without causing any power loss. On this basis, AD is advantageous over PD, confirming the preceding discussion. The larger K_c is, the better the damping effect is. Increasing K_c will cause a reduction in the inner loop bandwidth.

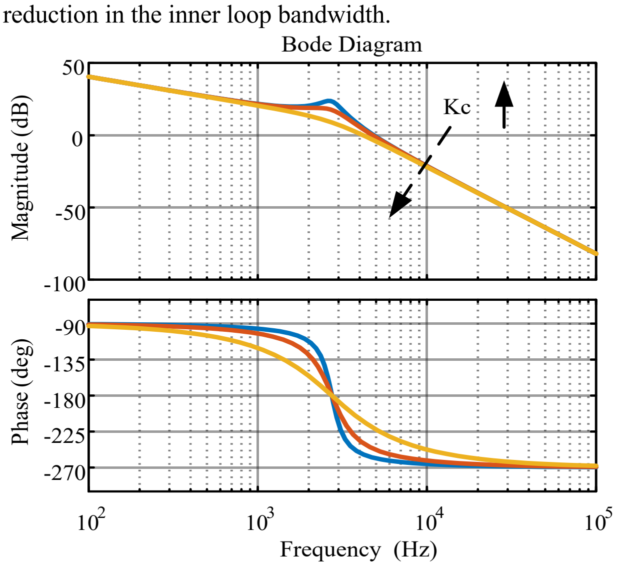

Fig. 7. Bode diagram of CCFAD for different Kc

(2) PR parameter design

After designing the inner loop parameter, the PR controller parameters should be selected. The impact of K_p, K_r, and ω_c on G_{PR} is shown in Fig. 8. K_p will affect the PR amplitude at all frequencies. In particular, the amplitude will increase as K_p is increased. On the contrary, K_r only varies the amplitude at frequencies around f_r. The resonant peak will increase as K_r is increased. The resonant bandwidth is influenced by ω_c. The larger ω_c is, the wider the resonant bandwidth is. In general, ω_c can be set to be π, given that grid frequency normally fluctuates in a small range [31]. In accordance with these characteristics, the PR controller parameters can be appropriately selected. The designed parameters for PR are K_c =0.2, K_p =0.09, and K_r =10. The corresponding bode diagram is shown in Fig. 9.

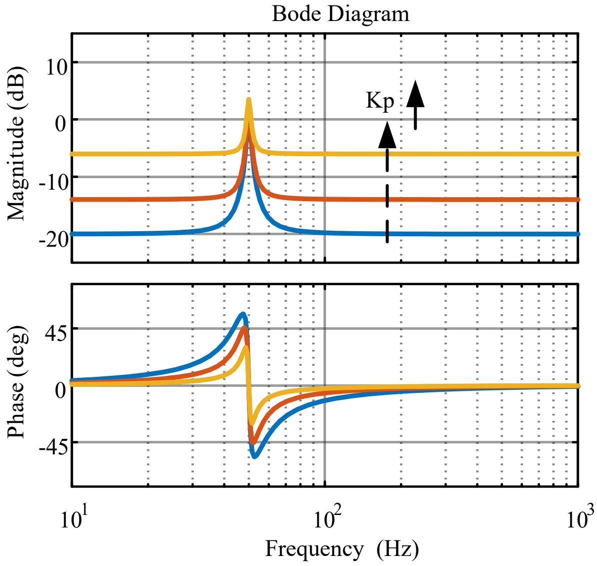

(a)

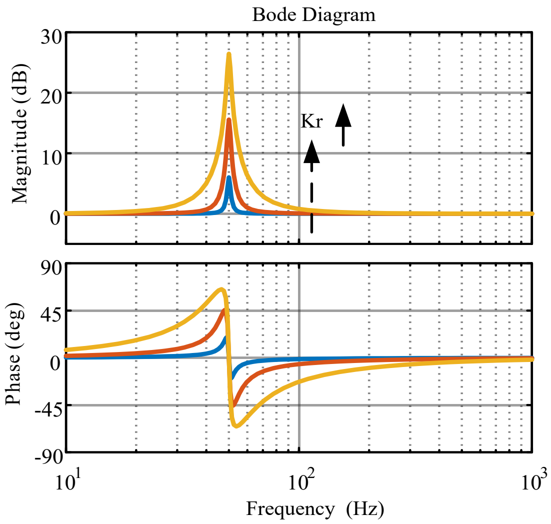

(b)

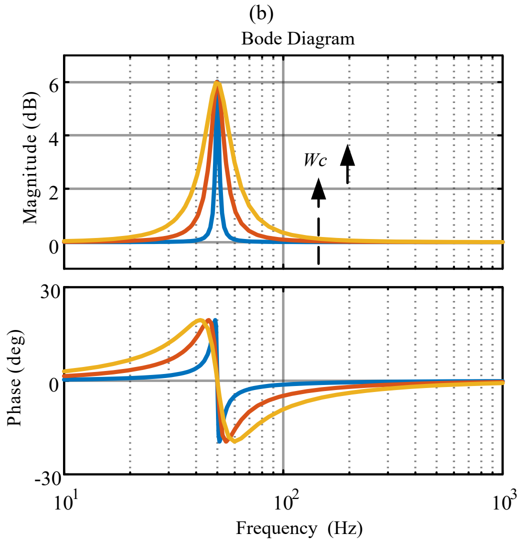

(c)

Fig. 8. Bode diagram of the PR controller for (a) different K_p, (b) different K_r, and (a) different ω_c.

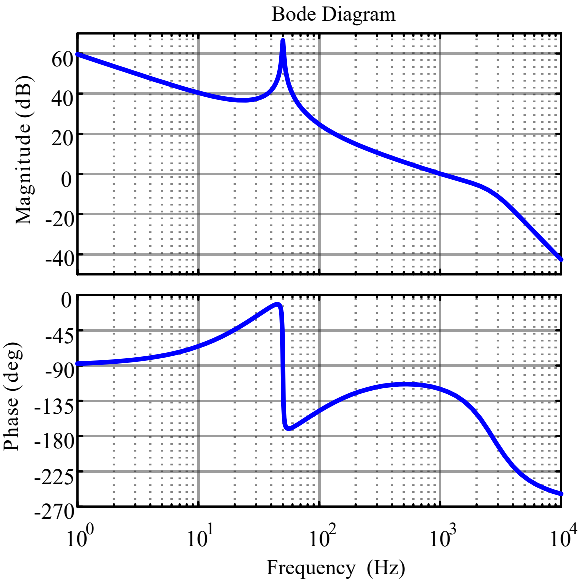

Fig. 9. Bode diagram of the GCI open loop.

4 Result Analysis and Discussion

To evaluate the performance of the proposed control strategy, several scenarios are simulated in the MATLAB/Simulink environment. Related parameters are listed in Table 1, and controller parameters are given as mentioned before.

Table 1. System parameters

Symbol	Parameter	Value
L_1	Inverter-side inductor	4.5mH
L_2	Grid-side inductor	1.5mH
C	Capacitor	3μF
V_{dc}	DC bus voltage	400V
f_{sw}	Switching frequency	10kHz
V_g	Grid voltage (RMS)	220V
f_0	Grid frequency	50Hz

4.1 Steady-state performance

To assess the control performance under steady state, the injected grid current is shown in Fig. 10, where i_{2_ref} is the grid reference current, and i_2 is the injected grid current. i_{2_ref} is well tracked by i_2. i_2 shows low current ripple and no distortion. That is, the injected grid current is in phase with grid voltage, inducing a high-power factor. Furthermore, CCFAD can effectively suppress resonance, ensuring system stability. The waveform also manifests the high performance of the proposed scheme based on PR and GVFF. Fig. 11 presents the resulting THD for injected grid current, which is equal to 2.33% and below 5%. This THD satisfies related IEEE standard. This finding demonstrates the performance of the advocated approach.

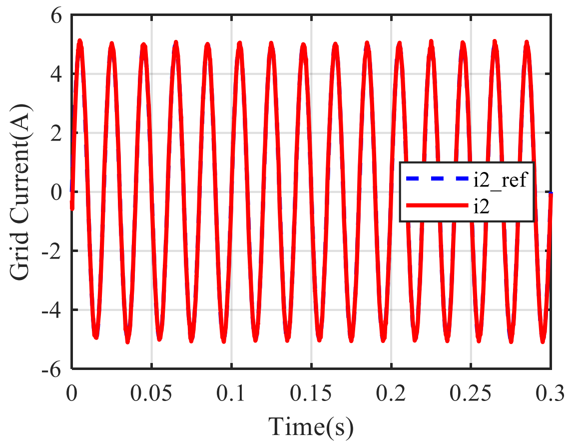

Fig. 10. Injected grid current waveform under steady state.

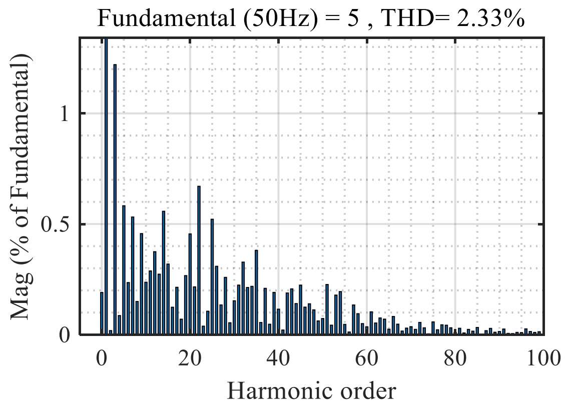

Fig. 11. Injected grid current THD under steady state.

4.2 Transient performance

The reference current with a step change is considered to examine the transient response by using the proposed method. The resulting response curve is displayed in Fig. 12, where i_{2_ref} is abruptly changed from 3 A to 6 A at approximately 0.15 s. i_{2_ref} curve is still well followed by i_2 curve, but without evident overshoot. Hence, the proposed approach shows a high dynamic response.

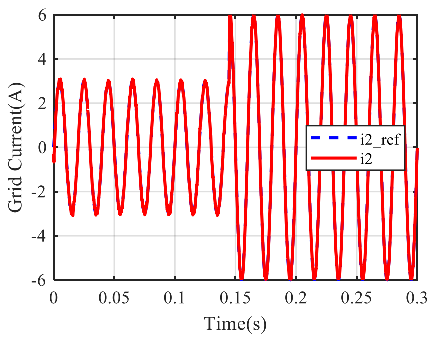

Fig. 12. Grid current waveform under step change.

4.3 Performance of GVFF control

Fig. 13 illustrates the injected grid current waveform by the proposed double-loop control but without GVFF. The injected current is relatively worse than that in Fig. 10. Owing to the absence of GVFF control, a large error exists between actual current and reference current in the first half cycle. This finding manifests the effectiveness of GVFF control.

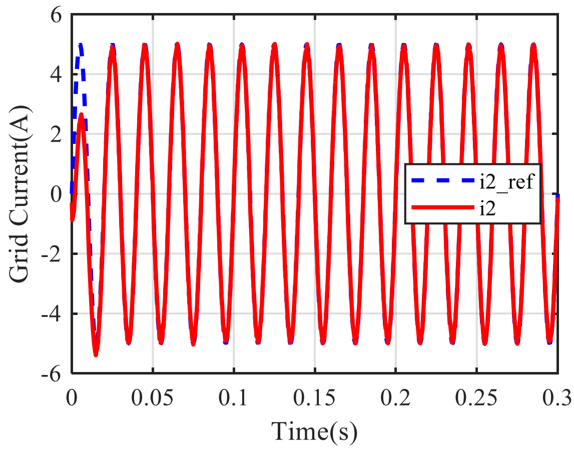

Fig. 13. Injected grid current waveform using control without GVFF

5. Conclusions

To obtain high-quality electric power for a generation system with SPGCI with an LCL filter, double-loop control with a GVFF-based control scheme is presented in this study. The resonant damping characteristics and a PR controller with parameter design are analyzed using a numerical simulation technique. The conclusions are drawn as follows:

(1) CCFAD can effectively suppress the resonant peak, ensuring system stability. It presents the advantages of simplicity and no power loss, leading to increased system efficiency.

(2) The PR controller can realize grid current control with such features as high steady-state accuracy, low THD, and fast response.

(3) GVFF control can enhance the fast tracking for grid current.

In this study, a dedicated scheme is presented to accomplish the control for SPGCI with an LCL filter via theoretical analysis and simulation experiment. CCF-based AD is recommended. Meanwhile, PR and GVFF control are combined to control injected grid current. The proposed approach is simple and effective and can be a design guideline for GCI control. Nevertheless, the situation for a weak grid is not considered. In view of this limitation, the future study can be conducted under a weak grid.

References

1. Aouchiche, N., “Meta-heuristic optimization algorithms based direct current and DC link voltage controllers for three-phase grid connected photovoltaic inverter”. *Solar Energy*, 207, 2020, pp. 683-692.
2. Shayestegan, M., Shakeri, M., Abunima, H., Reza, S., Akhtaruzzaman, M., Bais, B., Mat, S., Sopian, K., Amin, N., “An overview on prospects of new generation single-phase transformerless inverters for grid-connected photovoltaic (PV) systems”. *Renewable and Sustainable Energy Reviews*, 82(1), 2018, pp. 515-530.

3. Zhang, X., Tan, L., Xian, J., Zhang, H., “Predictive current control algorithm for grid-connected inverter with LCL filter”. *Transactions of China Electrotechnical Society*, 34, 2019, pp. 189-201.
4. Zhou, X., Lu, S., “A novel inverter-side current control method of LCL-filtered inverters based on High-Pass-Filtered capacitor voltage feed forward”, *IEEE Access*, 8, 2020, pp. 16528-16538.
5. Su, M., Cheng, B., Sun, Y., Tang, Z., Wang, H., “Single-sensor control of LCL-filtered grid-connected inverters”, *IEEE Access*, 7, 2019, pp. 38481-38494.
6. Zhang, J., Wang, M., “Passive damping control strategy of LCL-type PV grid-connected inverter”, *Chinese Journal of Power Sources*, 44(9), 2020, pp. 1334-1337.
7. Jo, J., Cha, H., “Design of effective passive damping resistor of grid-connected inverter with LCL filter for industrial applications”. *Journal of Electrical Engineering and Technology*, 14(5), 2019, pp. 2039-2048.
8. Albatran, S., Koran, A., Smadi, I., Ahmad, H., “Optimal design of passive RC-damped LCL filter for grid-connected voltage source inverters”. *Electrical Engineering*, 100(4), 2018, pp. 2499-2508.
9. Peña, J., Sampaio, L., Brito, M., Canesin, C., “RLC passive damped LCL single-phase voltage source inverter with capability to operate in grid-connected and islanded modes: design and control strategy”. *Electrical Engineering*, 102, 2020, pp. 2509-2519.
10. Xu, C., Wang, J., Bao, L., Deng, Y., “A novel design method of split-capacitor LCL filter”. *Power Electronics*, 55(07), 2021, pp. 39-45.
11. Xu, L., “Research on active damping control of voltage PWM inverter based on LCL filter”. *China Instrumentation*, 01, 2021, pp. 51-56.
12. Yang, X., Wang, T.,Xu, Y.,Yang, S., Li, H.,Mi, Y., “Voltage feed forward control of LCL grid-connected inverter based on virtual inductor”. *Acta Energiae Solaris Sinica*, 41(11), 2020, pp. 56-63.
13. Bierhoff, M., Soliman, R., Espinoza J., “Analysis and design of grid-tied inverter with LCL filter”. *IEEE Open Journal of Power Electronics*, 1, 2020, pp. 161-169.
14. Wu,H., Ding X., Qin, L.,“A current control strategy of single-phase LCL type grid-connected inverter based on dq coordinate system”. *Guangxi Electric Power*, 43(06), 2020, pp. 62-66.
15. Song G., Li G., Yang H., Li, H.，Chen Y., “Pi+State feedback controller of single-phase LCL pv grid-connected inverter based on d-q coordinate system”. *Acta Energiae Solaris Sinica*, 41(11), 2020, pp. 135-142.
16. Tang, X., Chen, W., Zhang, M., “A current decoupling control scheme for LCL-Type single-phase grid-connected converter”, *IEEE Access*, 8, 2020. pp. 37756-37765.
17. Geddada, N., Mishra, M., Kumar, M., “LCL filter with passive damping for DSTATCOM using PI and HC regulators in dq current controller for load compensation”, *Sustainable Energy Grids and Networks*, 2, 2015, pp. 1-14.
18. Dang, C., Tong, X., Song, W., “Sliding-mode control in dq-frame for a three-phase grid-connected inverter with LCL-filter”, *Journal of the Franklin Institute*, 357(15), 2020, pp. 10159-10174.
19. Zhu, D., Zou, X., Zhao, Y., Peng, T., Zhou, S., Kang, Y., “Systematic controller design for digitally controlled LCL-type grid-connected inverter with grid-current-feedback active damping”. *International Journal of Electrical Power & Energy Systems*, 110, 2019, pp. 642-652.
20. Eldeeb, H., Massoud, A., Abdel-Khalik, A., Ahmed, S., “A sensorless Kalman filter-based active damping technique for grid-tied VSI with LCL filter”. *International Journal of Electrical Power & Energy Systems*, 93, 2017, pp. 146-155.
21. Li J., Wu, X., Yi J., Luo, Y., “A control strategy for LCL-Type inverter based on improve double closed-loop state feedback”. *Power Electronics*, 51(09), 2017, pp. 68-70.
22. Sosa, J., Martinez-Rodriguez, P., Escobar, G., Vazquez, G., Valdez-Fernandez A., Martinez-Garcia J., “Analysis and validation for an inverter-side current controller in LCL grid-connected power systems”. *Journal of Modern Power Systems and Clean Energy*, 8(2), 2020, pp. 387-398.
23. Bighash, E., Sadeghzadeh, S., Ebrahimzadeh, E., Blaabjerg, F., “Robust MPC-based current controller against grid impedance variations for single-phase grid-connected inverters”. *ISA Transactions*, 84, 2019, pp. 154-163.
24. Young, H., Marin, V., Pesce, C., Rodriguez, J., “Simple Finite-Control-Set model predictive control of grid-forming inverters with LCL filters”. *IEEE Access*, 8, 2020. pp. 81246-81256.
25. Guzman, R., Vicuña, Ll, Castilla, M., Miret, J., Hoz, J., “Variable structure control for three-phase LCL-Filtered Inverters using a reduced converter model”. *IEEE Transactions on Industrial Electronics*, 65(1), 2018, pp. 5-15.
26. Benrabah, A., Xu, D., Gao, Z., “Active disturbance rejection control of LCL-Filtered grid-connected inverter using Padé approximation”. IEEE Transactions on Industry Applications, 54(6), 2018, pp. 6179-6189.
27. Yang, X., Sun, K.,He C., Grid connected Z-source inverter based on single cycle and dual current loop”. *Journal of Electric Power Science and Technology*, 36(02), 2021, pp. 155-161.
28. Zheng, F., Wu, W., Chen, B., Koutroulis, E., “An optimized parameter design method for Passivity-Based control in a LCL-Filtered Grid-Connected Inverter”. *IEEE Access*, 8, 2020, pp. 189878-189890.
29. Alamri, B., Alharbi, Y., “A framework for optimum determination of LCL-Filter parameters for n-level voltage source inverters using heuristic approach”. *IEEE Access*, 8, 2020, pp. 209212-209223.
30. Xu, J., Xie, S., Tang, T., “Improved control strategy with grid-voltage feed forward for LCL -filter-based inverter connected to weak grid”. *IET Power Electronics*, 7(10), 2014, pp. 2660-2671.
31. Yang, D., Ruan, X., Wu, H., “A real-time computation method with dual sampling mode to improve the current control performance of the LCL-Type grid-connected inverter”. *IEEE Transactions on Industrial Electronics*, 62(7), 2015, pp. 4563-4572.